Journal of Hydrology 537 (2016) 157–170

Contents lists available at ScienceDirect

Journal of Hydrology

journal homepage: www.elsevier.com/locate/jhydrol

Weekly variations of discharge and groundwater quality caused by intermittent water supply in an urbanized karst catchment

Felix Grimmeisen *, Moritz Zemann, Nadine Goeppert, Nico Goldscheider

Karlsruhe Institute of Technology (KIT), Institute for Applied Geosciences (AGW), Division of Hydrogeology, Kaiserstr. 12, 76131 Karlsruhe, Germany

ARTICLE INFO

Article history:
Received 23 October 2015
Received in revised form 31 January 2016
Accepted 21 March 2016
Available online 28 March 2016
This manuscript was handled by Laurent Charlet, Editor-in-Chief, with the assistance of Christophe Darnault, Associate Editor

Keywords:
Urban groundwater
Karst aquifer
Nitrate monitoring
UV–vis sensor
Correlation analysis
Jordan

SUMMARY

Leaky sewerage and water distribution networks are an enormous problem throughout the world, specifically in developing countries and regions with water scarcity. Especially in many arid and semi-arid regions, intermittent water supply (IWS) is common practice to cope with water shortage. This study investigates the combined influence of urban activities, IWS and water losses on groundwater quality and discusses the implications for water management. In the city of As-Salt (Jordan), local water supply is mostly based on groundwater from the karst aquifer that underlies the city. Water is delivered to different supply zones for 24, 48 or 60 h each week with drinking water losses of around 50–60%. Fecal contamination in groundwater, mostly originating from the likewise leaky sewer system is a severe challenge for the local water supplier. In order to improve understanding of the local water cycle and contamination dynamics in the aquifer beneath the city, a down gradient spring and an observation well were chosen to identify contaminant occurrence and loads. Nitrate, *Escherichia coli*, spring discharge and the well water level were monitored for 2 years. Autocorrelation analyses of time series recorded during the dry season revealed weekly periodicity of spring discharge (45 ± 3.9 L s^{-1}) and NO_3-N concentrations (11.4 ± 0.8 mg L^{-1}) along with weekly varying *E. coli* levels partly exceeding 2.420 MPN 100 mL^{-1}. Cross-correlation analyses demonstrate a significant and inverse correlation of nitrate and discharge variations which points to a periodic dilution of contaminated groundwater by freshwater from the leaking IWS being the principal cause of the observed fluctuations. Contaminant inputs from leaking sewers appear to be rather constant. The results reveal the distinct impact of leaking clean IWS on the local groundwater and subsequently on the local water supply and therefore demonstrate the need for action regarding the mitigation of groundwater contamination and reduction of network losses from sewer leakage. Furthermore, these investigations contribute to an improved understanding of urban water cycle systems in the Middle-East which may help water managers in the region to conserve precious resources.

1. Introduction

Worldwide, water managers of urban systems face severe challenges related to inefficient infrastructure. Urban areas and the process of urbanization strongly affect groundwater recharge processes in underlying subsurface layers and the quality of local natural water resources. Anthropogenic inputs and outputs create new water qualities and quantities through complex mixing processes accompanied by temporally and spatially highly variable dynamics (Lerner, 1986, 2002; Martinez et al., 2011; Schirmer et al., 2013). Large amounts of artificial recharge are thereby generated through leaks in water supply, sewerage, and storm drainage systems. This leads to contamination by effluents on the one hand and dilution effects by high losses of drinking water on the other hand (Eiswirth et al., 2004; Rutsch et al., 2006; Wolf et al., 2004). Commonly water mains losses in developed countries range from 5% to 25%, whereas in developing countries losses greater than 30% are common (Hibbs and Sharp, 2012). However, the urban environment makes it difficult to identify individual recharge sources, pathways and processes affecting the chemical and microbiological quality (Barrett et al., 1999; Vazquez-Sune et al., 2010). Leaky sewer and distribution networks are often closely spaced. Therefore, a mobilization of contaminants originating from sewage and dilution with drinking water leaking from the water supply pipes might occur at the same time.

Developing countries typically experience water scarcity and an increasing water demand due to population growth. In particular, urban centers nowadays establish a demand-based management instead of a supply based management (Vairavamoorthy et al.,

* Corresponding author. Tel.: +49 721 608 41926.
E-mail address: felix.grimmeisen@kit.edu (F. Grimmeisen).

http://dx.doi.org/10.1016/j.jhydrol.2016.03.045
0022-1694/

2008). Hence, the infrastructure of potable water and sanitation becomes an even more critical factor in the urban water cycle depending on the degree of inefficiency. In most developing countries, these circumstances have led water authorities to resort to intermittent water supplies (IWS). Here, a mostly regular, but interrupted water supply is forcing consumers to collect and store water for the non-supply hours and days (Hardoy et al., 2014; Kumar et al., 2013; McIntosh, 2003; Thompson et al., 2002).

Leaks from urban water supply systems are a major source of inefficient water infrastructure. Therefore, the IWS strategy, amongst others, is applied to reduce leakage losses. In the Middle East, the intermittent mode of water supply is an important factor contributing to the deterioration of potable water quality (Tokajian and Hashwa, 2003). Current literature on water quality of IWS has already illustrated the risk of contamination, which has many causes like supply rationing, polluted sources, leaky or poorly-functioning water storage, treatment or distribution systems (Kumpel and Nelson, 2013, 2014).

In Jordan, the sanitation systems are not sufficiently managed and provide ample potential for improvements towards sustainability. Leaky sewerage and water distribution networks are often an enormous problem. In most urban centers of Jordan, municipally-piped water is provided by a network of different distribution zones and is only intermittently available (for 12–60 h per week). Consequently, it is common practice to draw water off from the distribution system for the total duration of supply (Abu-Shams and Rabadi, 2003; Bonn, 2013; Rosenberg et al., 2008).

High population areas, such as Al Balqa or the cities of Amman or Irbid, are located in the mountains at the eastern margin of the Lower Jordan Rift Valley (LJV). Over history, these urban centers relied on groundwater from springs and shallow wells as sources of clean potable water (Suleiman, 2004). Karst aquifers dominate in these mountains in Jordan, and as well as in the Palestinian territories (West Bank) along the western margin of the LJV. A similar hydrogeology applies to Syria and Lebanon further north (Al-Charideh, 2011; Bakalowicz et al., 2008; Mimi and Assi, 2009). Regional water resources such as these have been exploited since historical times, but are nowadays often rendered unusable due to unregulated waste management (Amiel et al., 2010; Schmidt et al., 2013; Werz, 2006).

Karst aquifers are generally well known for responding rapidly to hydrological events, such as rainfall, but also to urban artificial recharge processes (Daher et al., 2011; Ford and Williams, 2007). Their focused flow and specific heterogeneity results in complex flow systems comprising dual or multiple porosities, that are characterized by a high susceptibility and vulnerability to pollution (Goldscheider, 2010; Gutierrez et al., 2014; White, 2002). Concentrated infiltration and rapid contaminant transport in the phreatic zone are characteristic, because karstified carbonates contain fast flow through conduits and enlarged fractures and slow flow components through the surrounding rock matrix (Atkinson, 1977; Schmidt et al., 2013; Toran and Reisch, 2013). This mixing of slow and fast flow components makes it difficult to determine pathways, residence times, and recharge areas. Protection of karst groundwater resources is notoriously challenging in urban settings.

In order to maintain a good groundwater quality, ambitious measures in water treatment and management have to be undertaken, such as protection zoning, reduction and fast detection of polluting activities. If practiced properly, permanent water-quality monitoring and contamination event detection is an inevitable measure for protection against pollutants and anthropogenic impacts.

This study focused on a karst aquifer contaminated with dissolved nitrate and fecal coliforms that underlies the city of As-Salt in Jordan. As-Salt had 88,900 inhabitants in 2011, and is located approximately 30 km northwest of Amman (Fig. 1a). As-Salt was founded about 300 BC and was the first capital of Jordan before Amman.

Two observations sites have been chosen for this case study. The first is a well that lies about 500 m down-gradient from the city center, and the second is Hazzir Spring that lies about 2.25 kilometers (km) down-gradient and represents resurgence from the karst aquifer. For a better understanding of the temporal variability of the contaminants, a spectrometric sensor for continuous high-resolution nitrate monitoring was installed. The nitrate sensor was combined with grab samples manually collected for fecal coliforms, including total coliforms and *Escherichia coli*. Dissolved nitrate is commonly used as an indicator for groundwater pollution (Fenech et al., 2012; Wakida and Lerner, 2005) and also frequently used as a monitoring parameter in karst studies (Huebsch et al., 2014; Katz, 2012; Panno et al., 2001).

The aim of this monitoring campaign was to improve the understanding of urban subsurface mixing processes and contamination dynamics in relation to discharge and groundwater level fluctuations. The study site can be considered as a blueprint for research into the impact of urban recharge processes controlled by leaky sewer and water distribution networks (specifically with IWS). To determine urban dilution and mobilization effects in groundwater, we considered high-resolution time series only for the dry season to avoid natural recharge impulses such as rain events. Time series of two summer seasons were studied by using correlation analyses on chemographs (spring nitrate and *E. coli*) and hydrographs (spring discharge and well water level). Correlation functions, such as autocorrelation, spectral analyses and cross-correlation, have already been applied many times to assess the relation between rainfall and discharge in karst systems (e.g. Fiorillo and Doglioni, 2010; Massei et al., 2006; Valdes et al., 2006; Zhang et al., 2013), but not for urban-influenced karst aquifers during dry periods.

2. Materials and methods

2.1. Study site

The Lower Jordan River Basin is characterized by a distinctive relief (416 m below and up to 1100 m above sea level) featuring a network of wadis distributed down the western slopes of the Transjordanian Mountains towards the LJV. Wadi Shueib is one of the sub-catchments, wherein the investigated springs' capture zone of approximately 4 km^2 is located (Fig. 1a). It lies in the upper part of the Wadi and is characterized by a rather steep valley with dense drainage network (Fig. 1b and c). The local climate is semi-arid with typical Mediterranean short rainy winter and long dry summer. Annual rainfall varies from approximately 500 to 700 mm.

Within this catchment, the city As-Salt is faced with severe water management problems due to several reasons. The water supply infrastructure is prone to high rates of losses and the average unaccounted for water (UFW) is estimated as 50–60% of the annual network supply, of which equal shares are assumed to physical and administrative losses due to metering failures (MWI and GTZ, 2004; Riepl, 2012). In As-Salt the water supply network is divided into 13 distribution zones which shift according to a weekly schedule. In each zone, water is available for 24, 48 or 60 h per week. In the area nearby the observation well and spring, the distribution network allocates five zones, that are supplied for 24 h (zone 1, 2), 48 h (zone 3, 4) and 60 h (zone 5) on different days of the week (Fig. 1d). The supply duration depends on the housing density, and no flow occurs in the distribution infrastructure

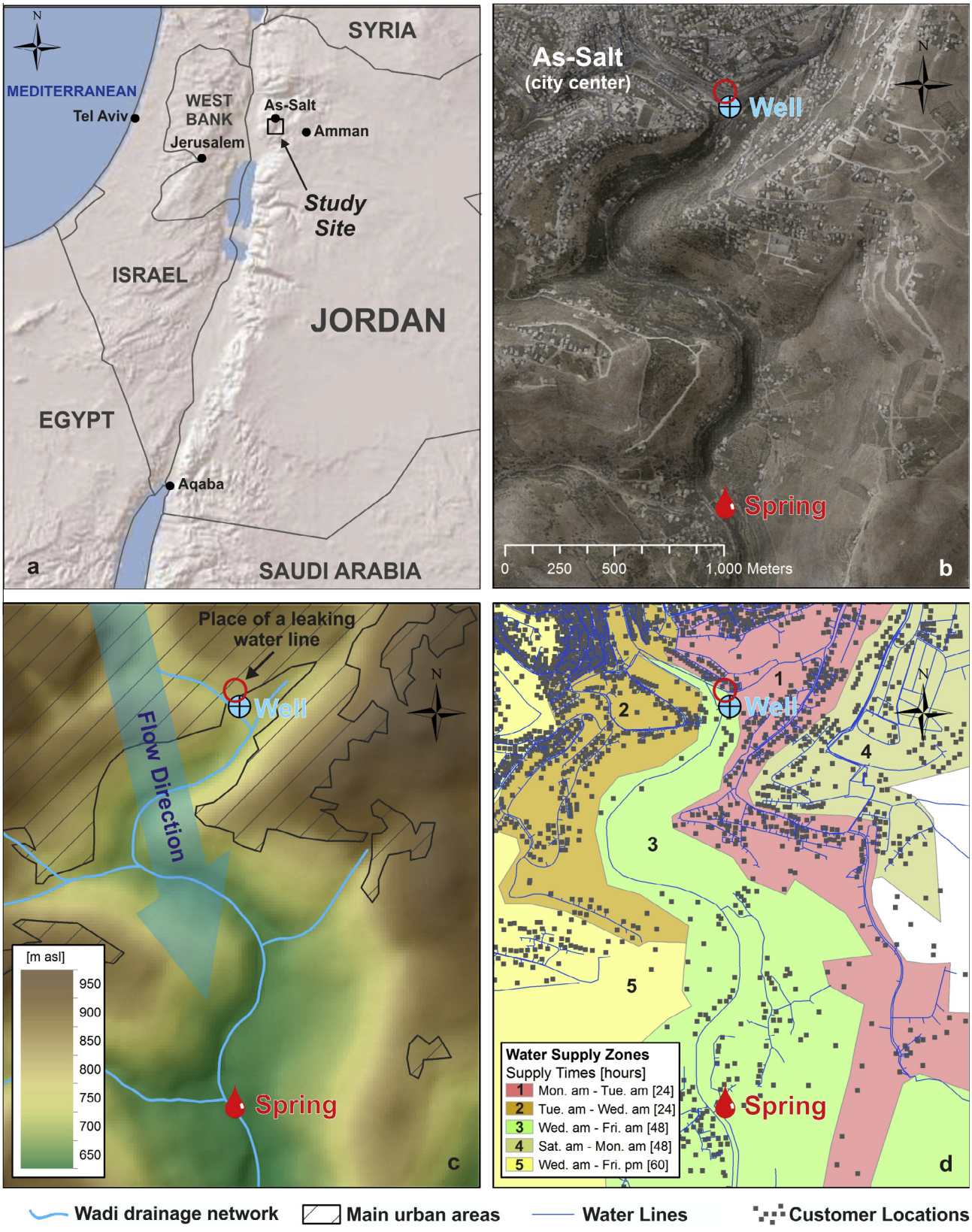

Fig. 1. (a) Location of the study site, (b) aerial view of the study site with Hazzir spring and observation well, (c) groundwater flow direction, (d) water supply zones of intermittent water supply. Figures (a–c) show also the place of a leaking water line (red circle) next to the well, which was detected during observations. (For interpretation of the references to color in this figure legend, the reader is referred to the web version of this article.)

during periods outside the supply times. Zone 1 and 2 include the city center with highest population and housing density.

Nearly 80% of households in As-Salt are connected to the sewer system that in parts probably dates back to the Ottoman period (1299–1922) (Al-Kharabsheh et al., 2013). About 25% of them use septic tanks which were often leaking due to porous walls and permeable bottoms (Margane et al., 2010). These rates also correspond to the average in Jordan (Van Afferden et al., 2010).

The aquifer is composed of Upper Cretaceous limestone–siltstone formations, which show complex tectonics with faults and deformations (Bender, 1968). Two formations outcrop in the area: the Amman Silicified Limestone, the Wadi Es Sir Limestone and the Wadi Shueib Formation (Moh'd and Muneuzel, 1998). The two limestone units form the major karst aquifer, consisting of thinly bedded limestones, alternating with massive limestones containing nodular cherts (Ta'any, 1992). The aquifer is drained by contact springs which occur at the boundary of the underlying aquitard, calcareous marls of the Wadi Shueib Formation, or by overflow springs at steep faults (Abu-Jaber et al., 1997; Hahne et al., 2008). In the study area, the thickness of the aquifer ranges from 90 to 100 m. Natural recharge occurs in the mountain regions where the layers are exposed and well karstified (Flexer and Yellin-Dror, 2008). Regionally, these aquifer systems are of great importance due to considerable recharge rates via surface infiltration and subsequently rapid drainage through a karstic conduit network. Literature data on the hydraulic conductivity of the main aquifer (Wadi Es Sir) ranges from $2 \cdot 10^{-5}$ to $1 \cdot 10^{-3}$ ms^{-1} (Geyh et al., 1985; Margane et al., 2002; Parker, 1970).

The perennial Hazzir Spring is located 2.15 km south or downstream of the city center at the foot of the eastern slope close to the Wadi Shueib (Fig. 1b and c). The spring is captured in a concrete reservoir and flows in a channel towards the creek. The total annual discharge is reported at 1.3 million m^3 or about 40 L s^{-1}; (Margane et al., 2010). The spring was used for drinking water supply for several decades. However, due to frequent contamination with fecal bacteria, the spring has been disconnected from the water supply system since 2012. Before 2012, occasional interruptions of supply took place mainly after rain events, due to the rapid increase of turbidity which caused technical problems for membrane filtration at the treatment plant. After membrane filtration, raw water is permanently treated by chlorination for disinfection. In general, a distinctive response to hydrological impulses in terms of water quality and quantity is a well-studied feature in karstic environments (e.g. Geyer et al., 2008; Pronk et al., 2006).

In 1999, a 194-m deep borehole with diameter of 300 mm was drilled in As-Salt (Fig. 1b–d). Located about 100 m north of the drainage network, it was originally planned as a water-supply well. Owing to unacceptably small flow rates and poor water quality, the borehole was converted into a monitoring well, the only one in the city. The well intersects three stratigraphic formations: the Wadi Es Sir Limestone, marls of the Wadi Shueib Formation and limestones of the Hummar Formation, which include a deeper confined karst aquifer system.

The exact thickness of the formations and the dimensions of the casing screen at the well are not known. In the upgradient catchment area of the observation well, one well at 2.3 km distance and a well field (5 wells) at approximately 3.6 km distance are permanently used as water supply for As-Salt. Zemann et al. (2015) illustrate the location and stratigraphic intersection of these wells. The well is located only about 60 m away from a leaking water line. The water table in the well is influenced by inflowing water, which can even be recognized by a splashing sound. The leaking water line is a main pipe for distribution in zones 1 and 2. Therefore, the water line is weekly pressurized for 48 h contiguously, because water supply in zones 1 and 2 corresponds in sum to the period from Monday a.m. to Wednesday a.m.

The municipal area of As-Salt lies at 800–1000 m asl directly within the groundwater contribution zone of the spring and the well and therefore poses a persistent risk to water quality. Agricultural activities are of minor relevance, as the crop areas consist of only few small plots. Steep relief does not allow for more facilities (Riepl, 2012).

The constant degradation of the spring water quality has been well documented for two decades (Abu-Jaber et al., 1997; Al-Kharabsheh et al., 2013; Margane et al., 2010). In addition to contamination with coliform bacteria, dissolved nitrate concentrations greater than the maximum admissible concentration (MAC) of 50 mg/L NO_3 of the Jordanian Standard for drinking water have been reported.

2.2. Spring discharge, water level in monitoring well, and sampling data

2.2.1. Sensor measurements

High-resolution monitoring of nitrate in spring water was performed with a multiple wavelength spectrophotometer probe between 01/03/2012 and 04/12/2013 at 15 min intervals. The sensor (spectro::lyser™, s::can Messtechnik GmbH, Austria) with 35 mm measuring path was installed together with an autocleaning system of pressurized air at the spring resurgence. The sensor continuously measures the absorbance of electromagnetic radiation in the ultraviolet and visible wavelength range from 200 to 750 nm with a resolution of 2.5 nm (=256 single measurements). The wavelengths between 205 and 240 nm are taken for nitrate evaluation by using derivative spectroscopy and deconvolution algorithms (Bende-Michl and Hairsine, 2010; Huebsch et al., 2015; Perfler et al., 2006). The nitrate-nitrogen concentration is computed (NO_3 [mg N L^{-1}]) following the Lambert–Beer law for dilute and homogeneous solutions. Because each water body comprises a distinctive fingerprint in terms of natural interferences by its background matrix, a particular calibration procedure was set. Organic matter, carbonate and humic acids (amongst others) naturally interfere with different magnitudes owing to absorbing light in the same spectral range as nitrate (Krockel et al., 2011).

In addition to the global calibration of the sensor (=factory setting based on lab standard solutions) an on-site calibration was performed by using spring water. For that reason pure water or a 1 M nitrate standard was added to spring water to mix four calibration solutions, two by dilution and two by concentration, respectively. Calibration samples were analyzed in the laboratory by ion chromatography (Dionex ICS-2100, Thermo Scientific, Finland). The calibration line was computed with a second-order polynomial function. The nitrate-nitrogen concentrations of the five calibration samples range from 6.1 to 18.1 mg L^{-1}. The correlation coefficient for nitrate-nitrogen concentrations of lab analyses and the calculated UV–vis sensor concentrations was $R^2 = 0.976$ after on-site calibration (Fig. 2a), compared to $R^2 = 0.851$ after global calibration. The error range of sensor nitrate measurements is determined by the manufacturer's specification of the expected concentration interval which is "0.02 · measured concentration + 1/path length of the sensor".

Nitrate concentrations observed with the UV–vis sensor were compared to nitrate concentrations determined in the laboratory. To verify the UV–vis sensor measurements, 47 samples were taken and nitrate concentrations analyzed to evaluate long-term accuracy (Fig. 2b). In March (23 samples), May to June (12 samples) and November 2013 (12 samples) three campaigns were performed. The samples were filtered using a 0.45-μm micropore membrane, 6 samples were kept unfiltered to determine the influence of organic substances. Before analyses, all samples were stored at 4 °C, except for 6 h travel by airplane and train.

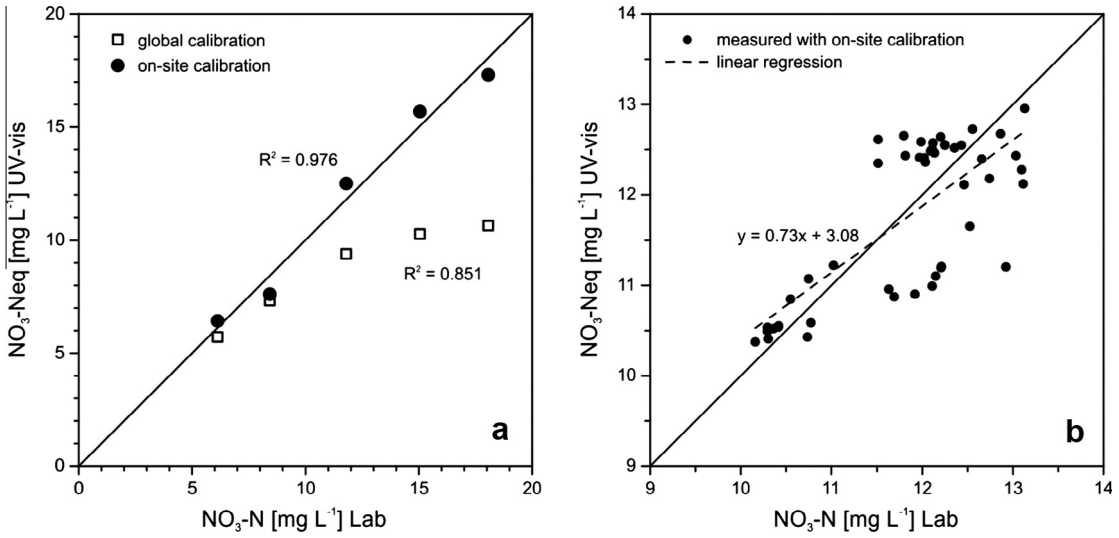

Fig. 2. (a) Validation of the on-site calibration of the UV–vis sensor; (b) accuracy of the used on-site calibration of samples measured in 2013.

Spring discharge was determined with a V-notch weir in the channel next to the spring outlet (e.g. Goris, 2012). The water level was measured by an ultrasonic sensor at 15 min intervals (NivuMaster, Nivus GmbH, Germany) attached 80 cm upstream from the weir. Due to the course of the spring channel upstream of the weir the flow attained no ideal waveless conditions to measure the water level and little waves continuously disturbed the signal. Margane and Zuhdy (1995) documented an average spring discharge for the years 1983–1993 of 40.7 L s^{-1}.

Monitoring of groundwater level at the observation well was performed by using pressure transducers (CTD-Diver and Baro-Diver, Eijelkamp, Netherlands) at 15 min intervals. The time period monitored was between 09/06 and 04/11/2013. Groundwater level data was compensated for barometric pressure.

Generally in the study area only few but intense rain events occur during the rainy winter season, often more than 50 mm within 24–48 h, and followed by flood waves through the wadi (Schmidt, 2014). In earlier investigations (unpublished) it was observed that at the observation well and Hazzir Spring, water level or discharge and water quality respond fast and within 20–24 h after precipitation. Subsequently, e.g. when the spring discharge rises, the water quality usually shows a strong increase of turbidity and bacteriological contamination (*E. coli* > 5.000 MPN 100 mL^{-1}), which is generally a well-known hydrologic feature of karst aquifers.

The duration of time series used for correlation analyses is 274 days (05/03–05/11/2013) for the spring and 148 days (09/06–04/11/2013) for the well.

2.2.2. Sample data

The general goal of the sampling campaigns was to identify high-impact contamination events. For water suppliers, it is important to react rapidly after a contamination event. Therefore during the summer period of 2012 and 2013, two water qualities sampling programmes were carried out to determine the urban impact on *E. coli*. Water samples were collected at the spring tub outlet for 11 days in September 2012 and 17 days in May to June 2013. Samples for microbial analysis were collected in 100 mL bottles containing sodium thiosulfate, and tests were performed either immediately or samples were stored in a refrigerator at 4 °C and tested within 10 h. In total 56 samples were tested. Bacteria were identified by the most probable number (MPN) per 100 mL (MPN 100 mL^{-1}) following the Colilert-18 Quantitray 2000 method (IDEXX Laboratories Inc. Westbrook, U.S.A.). Samples were incubated at 35 °C and counted after 18–22 h. The microbial detection range of the testing method is from 1 MPN 100 mL^{-1} to 2419.6 MPN 100 mL^{-1} (substituted with 2.420 MPN 100 mL^{-1}). *E. coli* values are log transformed using $\log_{10}(x+1)$. The samples exceeding the upper bound of detection were tested again at a dilution factor of 1:10 (with additionally stored water and 18–22 h after first testing). Although the dilution of samples and its statistical approach of counted rates by the Colilert® testing method is not validated by the manufacturer, it approximates the rough levels of contamination above the upper bound.

2.3. Data analysis

2.3.1. Sensor data evaluation

This study followed the data evaluation method used in Rieger et al. (2006) for dissolved nitrate, where the accuracy of the UV–vis sensor measurements was verified. To compare the precision of the sensor with the laboratory analyses, a residual standard deviation (s_x) and the coefficient of variation CV_x was calculated using Eq. (1):

$$s_x = \sqrt{\frac{\sum_{i=1}^{n}(x_i - \bar{x})^2}{n-2}} \quad [\text{mg N L}^{-1}] \tag{1}$$

where n is the number of measurements, x_i is each individual measurement and $\bar{x}$ is the sample mean.

To compare two different measuring devices (online sensor and laboratory) with different working ranges, the residual standard deviation is standardized by dividing by the mean laboratory value. CV_x is a relative measure of precision.

$$CV_x = \frac{s_x}{\bar{x}} \cdot 100 \ (\%) \tag{2}$$

2.3.2. Time series analysis

The time series of spring discharge, nitrate concentration and the well water level from the summer season 2013 are used to determine the frequency content of the signals and the relation between the time series by using autocorrelation and cross-correlation. Since correlation analysis in hydrology was established by Mangin (1984), Box et al. (1994) and others, it was applied in many studies on karstic aquifers (e.g. Fiorillo and Doglioni, 2010;

Larocque et al., 1998; Massei et al., 2006; Padilla and Pulido-Bosch, 1995; Slimani et al., 2009; Valdes et al., 2006).

2.3.2.1. Autocorrelation function and amplitude spectra. As a first step, the autocorrelation function of each signal is calculated. The autocorrelation function $r_{xx}(k)$ characterizes the linear dependence of successive values over a time period and is estimated as normalized measure:

$$r_{xx}(k) = \frac{1}{(n-k)\sigma^2}\sum_{t=1}^{n-k}(x_t - \bar{x})(x_{t+k} - \bar{x}) \quad (3)$$

where k is the time lag ($k = 0$ to m), n is the length of the time series, σ^2 the variance, x is a single event, $\bar{x}$ is the mean of the events, and m is the truncation point. Each time series was autocorrelated to itself for increasing time lags. The autocorrelation function highlights the amplitude of pre-existing periodicities in the time series. To determine whether the autocorrelation coefficient at lag k is significantly different from zero and is not considered as noise, most authors used the value of the lag time that corresponds to 0.2. However, several karst studies demonstrated that any value of the autocorrelation, if reasonable, could be chosen (Massei et al., 2006).

As a second step, the spectral density functions (amplitude spectra) of the autocorrelation functions were calculated, which can be obtained by fast Fourier transform (FFT). The amplitude spectrum describes the frequency domain of what the autocorrelation function expresses in the time domain. Through the identification of different peaks in the amplitude spectra, the dominating periods of the phenomena are represented. This helps to characterize the system. Furthermore, the different modes of variability of the time series are compared and interpreted in terms of structural organization (karst features, intensity and attenuation).

2.3.2.2. Cross-correlation function. As a third statistical step, cross-correlation analyses were performed. Cross-correlation is most appropriate to compare two time series that may have a temporal dependency (Davis, 2002). Cross-correlation analysis is applied to determine transformations in the karst aquifer of an input function (usually precipitation) and the coherent output functions (e.g. time series of well water level, spring discharge and nitrate concentration). Computing the cross-correlation function $r_{xy}(k)$ between the input function $x(t)$ and the corresponding output function $y(t)$ is equivalent to the autocorrelation function, but the signal is correlated with a different signal:

$$r_{xy}(k) = \frac{C_{xy}(k)}{\sigma_x \sigma_y} \quad (4)$$

where $C_{xy}(k)$ is the covariance between the input signal x_i and the output signal y_i, computed at the time lag k, with the standard deviations σ_x and σ_y of the time series. A cross-correlation analysis provides information on the causal and non-causal relationships between the input and the output as well as the importance of these relationships (Liu et al., 2011). The cross-correlation function is not symmetrical and if $r_{xy}(k) > 0$ for $k > 0$, the input influences the output. The values of $r_{xy}(k)$ range between -1 (perfect negative correlation) and +1 (perfect positive correlation). The corresponding lags represent the sense of movement of one time series past the other. A positive lag of significant correlation coefficients signifies the delay of the output function, whereas significant correlation coefficients of negative lags implicate an output signal influencing the input signal.

Cross-correlation analysis can verify whether a (well-organized) karstic network quickly drains the aquifer. It shows whether the karstic network is exclusively or only partially the main receptive part during varying flow conditions. This is expressed by a more or less attenuated correlation coefficient and the corresponding delay. Usually, the shorter the delay of an impulse (input function), the faster the transfer within the karstic network and the less the corresponding lag.

In this study, the input functions employed are based on the operating supply periods of the intermittent water supply system in the study area. As the signals cannot be measured directly, the input time series are computed, which appear with regular intermittency. Therefore, the information of weekly supply periods in the zones encompassing the nearby catchment upstream of the spring and well are used (Fig. 1). The input time series therefore was a simple step function representing the supply cycle in the drinking water network using only two values, one for supply and one for no supply.

For simplification of the input signal the time series were computed by assuming one constant supply signal during operation. In comparison, a more realistic signal corresponding to a regular pumping cycle would not be constant but probably more similar to a breakthrough curve with long tailing (with pressure peak in the beginning for flushing). The length and intervals (15 min) of the computed input time series equals the well and spring time series.

3. Results and discussion

3.1. Time series

Fig. 3 illustrates the spring discharge and dissolved nitrate concentrations and the well water level time series for low flow conditions in summer 2013. Time series for summer 2012 are shown in the Supplementary material. Between March and November 2013, only 3 minor precipitation events were recorded at As-Salt: 17/03 (4.0 mm), 05/04 (3.6 mm) and 17/04 (1.2 mm) based on data from the climatic station on the roof of the water supply building next to Hazzir spring. These small precipitation rates did not lead to significant responses at the spring or well. Therefore the illustrated observations are considered as high-resolution time series during low-flow conditions.

3.1.1. Spring discharge

The unsmoothed discharge time series varies between 25 and 60 L s^{-1} and is characterized by a noisy signal owing to the non-ideal installation of the ultrasonic sensor and the effect of the disturbed water surface in the spring channel. A 96-points (4 readings per hour × 24 h = 96), symmetrical smoothening (=1 day smoothed) leads to a better interpretation of spring discharge, since misleading erroneous single measurements are reliably suppressed. These misleading single values are most likely minimum and maximum values amongst others, and therefore not trustworthy. The smoothed discharge time series varies approximately between 37 and 52 L s^{-1}. Discharge does not show a general decreasing or increasing trend over the period, but is rather constant at an average level of 45 L s^{-1} (±3.9 standard deviation). It is further characterized by a regular weekly oscillation pattern. Due to its regular occurrence, this signal is assumed to be not natural. The discharge is quite constant over season, which is also non-natural, since spring discharge is usually supposed to decrease, when there is no rainfall. It points to the influence of artificial recharge. The derived average spring discharge nearly confirmed measurements documented in literature of approximately 40 L s^{-1} (1983–1995, Margane and Zuhdy, 1995), and shows rather a slightly increased level.

3.1.2. Nitrate concentrations

The time series of nitrate concentrations expressed as NO_3-N start at about 12.5 mg L^{-1} (55.4 mg L^{-1} NO_3^-) and follow a slightly decreasing trend towards about 10 mg L^{-1} at the end. Similar to

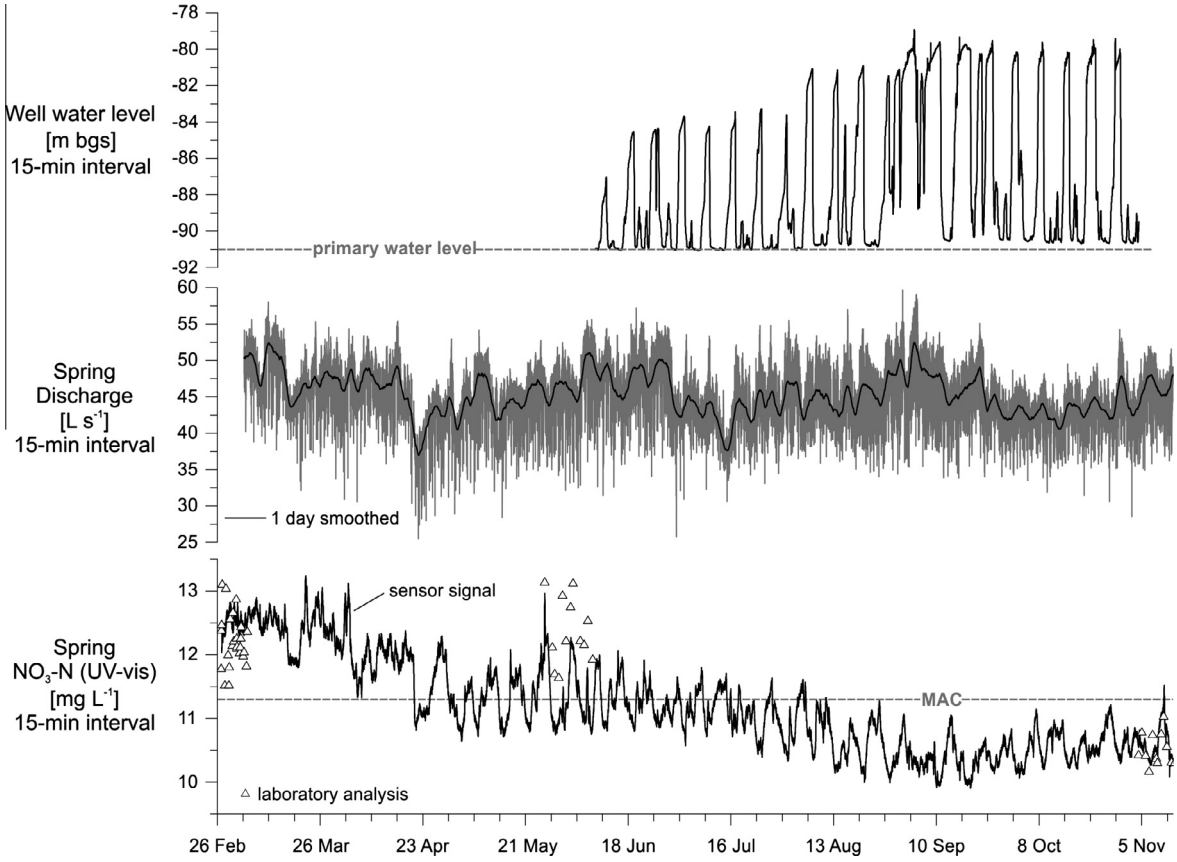

Fig. 3. Spring discharge and nitrate time series from March to November 2013 and well water head time series from June to November 2013. MAC = maximum admissible concentration of nitrate (NO_3-N) at 11.3 mg L^{-1} (50.0 mg L^{-1} NO_3^-).

discharge, it also shows distinctive variations on a weekly basis (Fig. 3). Generally the concentrations vary with an average of 11.4 mg L^{-1} ± 0.8 standard deviation and an error range of 0.03 mg L^{-1} of the sensor. In comparison to lab analyses, the coefficient of variation is 7.4% with an accuracy of 0.57 root mean square error (Fig. 2b).

As nitrate contamination in groundwater is well established to indicate agronomic or urban activities in the catchment, its importance is mostly associated with the maximum admissible concentration (MAC). In Jordan the MAC for nitrate is 11.3 mg L^{-1} NO_3-N (50 mg L^{-1} NO_3) (Margane et al., 2010). The nitrate concentrations are consistent with the previously-known contamination problem of the spring. Zemann et al. (2015) reported on groundwater pollution which is attributed to urban sources such as sewer and septic system leakage.

According to Peterson et al. (2002) and Huebsch et al. (2014) nitrate concentrations are supposed to remain relatively constant if either a large groundwater storage is present, or groundwater flow is dominantly diffusely organized or is observed during base flow conditions only. Although nitrate in this study varies only by 7.4%, its distinct weekly variation pattern points to an urban influence and to relatively fast pathways in the aquifer even under low-flow conditions.

3.1.3. Well water levels

The groundwater level at the observation well is also characterized by frequent and regular fluctuations. It shows one rather constant lower level at 91 m below ground surface (bgs), which suggests that it may be the potentiometric surface at low water for the confined deeper karst aquifer. Besides, the time series is interrupted by superimposed weekly peaks (Fig. 3). These peaks are characterized by a rising trend in the peak levels over time. Starting with a first and abrupt rise of approximately 4 m in one day, the peak level reaches fluctuations of 10–11 m. Furthermore, between the regular and distinctive pattern of the peaks, the time series shows also shorter and smaller peaks of a few hours.

Principally this well water level time series does not show a natural pattern of groundwater level fluctuations, because it represents a "natural" plateau low water level on the one hand and an artificial high water level on the other. The low-yield well appears to tap only one deeper confined karst aquifer, below a sequence of weakly karstified limestones and marls, represented by a relatively constant potentiometric surface. Furthermore the time series highlights some short-term functioning of a karst network, represented by variations within 24 h and the non-natural intermittent pattern. The principal cause of the observed fluctuations is assumed to derive from substantial leakage(s) from a nearby water line, pressurized on a weekly basis due to IWS (Fig. 1b–d). A potential impact of a weekly pumping regime of a water supply well is unlikely, since the nearest supply wells are more than 2 km upgradient, and also not terminated on a weekly basis.

Fig. 4 presents a conceptual model of the close area of the observation well and the local hydrostratigraphy. The weekly increase of the potentiometric surface was induced by periodic percolation of leakage water from a nearby defective water line to the urban center As-Salt, which was found in approximately 60 m upgradient of the well.

3.2. Autocorrelations and amplitude spectra

Fig. 5 presents the autocorrelation functions of the three time series (spring discharge, spring nitrate and well water level). The

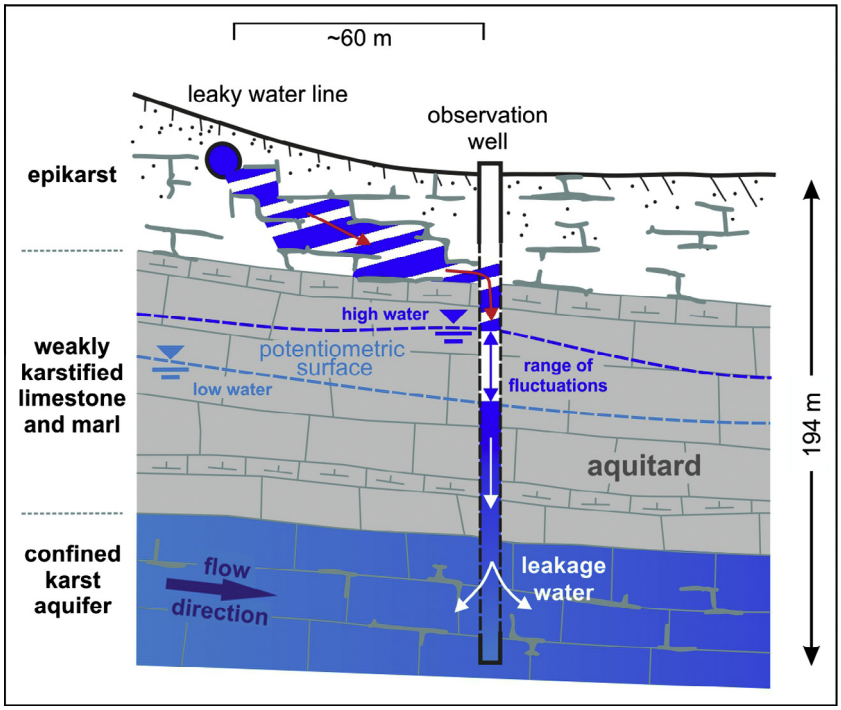

Fig. 4. Simplified conceptional model of the observation well and the local hydrostratigraphy. The well taps a confined karst aquifer. Potentiometric surface indicates weekly fluctuations with a range of 4–11 m due to leakage of a nearby water line, pressurized on the basis of IWS.

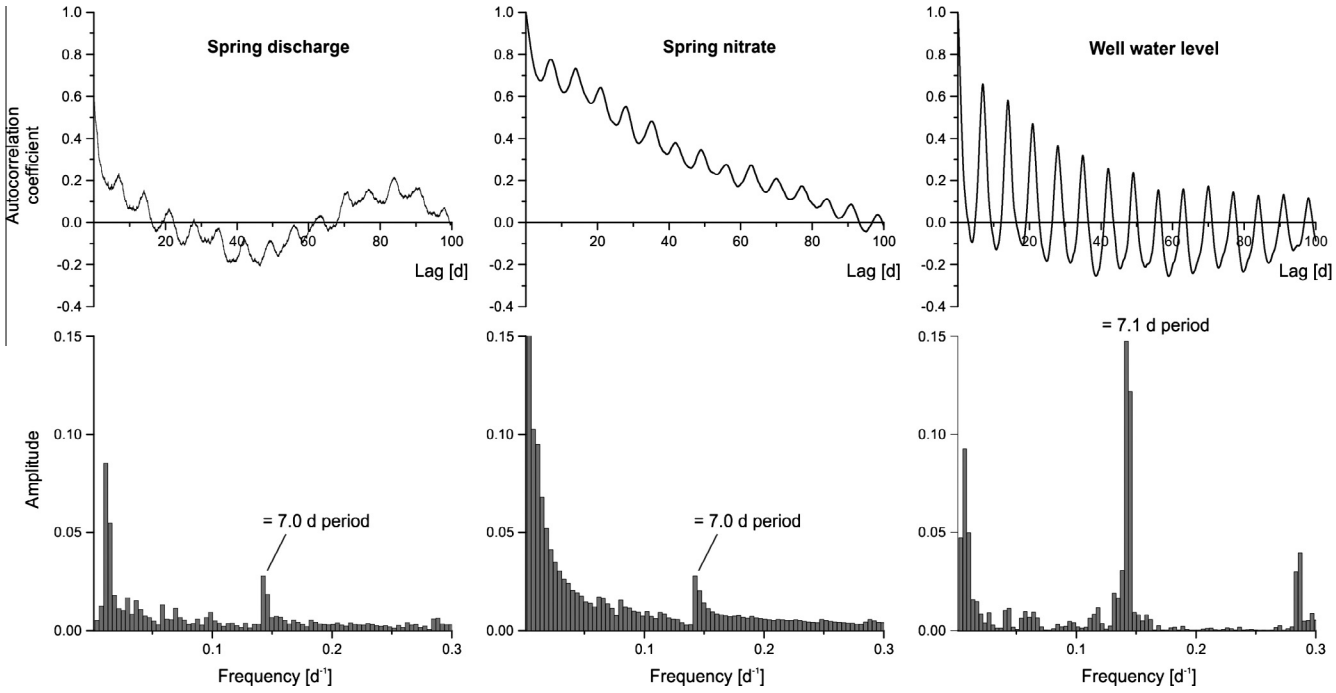

Fig. 5. Autocorrelation functions of discharge and nitrate time series of the spring and the well water level time series and corresponding energy spectra computed by fast Fourier transform. A pre-existing conspicuous periodicity in each signal is particularly expressed at the frequency 0.14 d^{-1}, which equals a 7-days or weekly period.

autocorrelation functions are all characterized by distinctive periodicities with a similar oscillation corresponding to a phase of approximately 7 days. The amplitudes of spring discharge and nitrate are similar, whereas the well water level autocorrelation function is sharper and with stronger amplitude. The magnitudes of the different pre-existing periodicities in each signal are expressed by the autocorrelation coefficient.

The autocorrelation function can describe and highlight information (e.g. periodicities) or a memory effect (e.g. rainfall events) of an output signal without knowing the magnitude or existence of one or more input signals (Massei et al., 2006). It is a way to interpret the complex information of a time series, as it corresponds to the overall shape and magnitude of the autocorrelation function rather than just a single value.

Inasmuch as the autocorrelation functions clearly express the periodic components in the signals, the amplitude spectra are used to compare the frequency content of the time series. The calculated frequencies are illustrated in Fig. 5 below the three functions. Spring discharge and nitrate concentration as well as well water level show an evident structure, with distinctive peaks. In all three amplitude spectra, 2–3 spectral components can be distinguished. Approximately at 0.14 d^{-1}, a distinct peak is present in all three spectra, expressing a periodicity of 7 days. Peaks of less than 0.2 d^{-1} (>50 days periodicity) are detectable as well, representing the possible long term (e.g. seasonal) periodicity of the signal. Since time series of only one summer period are computed, these frequencies were not further evaluated in this study. The third weaker peak at 0.28 d^{-1} of the well water level spectra equals a 3.5 days periodicity and characterizes the smaller peaks between the distinct weekly peaks of the well water level time series (cf. Fig. 3). The described content of all three output signals indicates the existence of a weekly input signal transferred through a hydrologic network of the local karst aquifer system. This information at a small scale highlights the short-term functioning of the karst network.

3.3. Occurrence of fecal bacteria

The levels of detected *E. coli* during the two sampling campaigns at the spring in September 2012 and May to June 2013 are summarized in Table 1 and illustrated in Fig. 6, where detection rates are combined with dissolved nitrate concentrations. The background color of Fig. 6 is accompanied with a color gradient that helps to better visualize the weekly pattern. In all groundwater samples, *E. coli* were present at high detection rates. *E. coli* showed detection rates with 5 samples exceeding the upper bound at 2.420 MPN 100 mL^{-1} and lowest rates at about 50 MPN 100 mL^{-1} (average: 713 MPN 100 mL^{-1}).

Within the period of sampling, nitrate concentrations showed weekly fluctuations with peaks of 12–13.5 NO_3-N mg L^{-1} during Sundays to Tuesdays (~48 h period) and minima periods with values about 11 NO_3-N mg L^{-1} during Wednesdays to Saturdays. The temporal evolution of *E. coli* shows in September 2012 a slightly gradual pattern with rather disordered variations and a proper curve progression in May to June 2013. Highest rates of *E. coli* were detected in Sunday samples in September 2012 and in Sunday/Monday samples in June 2013. Lowest rates of *E. coli* were detected in Tuesday/Wednesday samples of September 2012, generally in May (Monday to Saturday) and Thursday to Friday in June 2013.

Although a low *E. coli* rate of about 50 MPN 100 mL^{-1} occurred also on a Monday, May 27th 2013, highest levels of contamination were detected on Sundays to Mondays, whereas lower rates of detection occurred mainly between Tuesdays and Fridays. As shown in Fig. 6, particularly in June 2013, the *E. coli* follow the weekly pattern of nitrate, although the fluctuation of nitrate is rather small with a range of approximately 1.5–2 mg L^{-1}. Overall, *E. coli* show a temporal pattern similar to nitrate. Therefore both substances are likely to originate from the same source.

3.4. Cross-correlation functions

Cross-correlation functions were used to further assess the detected weekly variations of spring discharge, spring nitrate, and well water level. This analysis provides a better understanding of the spatial and temporal urban impacts which trigger weekly variations in the highly susceptible karst aquifer system. In particular, it is important to show whether a constant background level of contamination is periodically diluted by another source of clean water, or whether periodic pulses of contaminants increase the level of pollution. The use of cross-correlations helps to evaluate the degree of similarity and the temporal relationship between an input and an output signal, but in this study, a missing input signal limits the analysis. Therefore it is necessary to identify the input signal that might cause the weekly variations.

The measured output signals comprise an approximation of an enduring anthropogenic input signal which contains weekly variations. Local network losses from water mains are supposed to induce distinct hydraulic impulses since they recur at fixed locations in a supply zone when the lines are charged with water. For the cross-correlations applied, step function input signals were used which approximate the schedule of the intermittent water supply in one supply zone.

These simplified signals refer to alternating periods of no flow in the water supply lines (value 0), and thus no leakage, and the weekly period for a functioning water supply with pressurized lines (value 1), and thus a leakage to the karst aquifer. In total three different supply (input) signals were computed. Fig. 7a shows

Table 1
Summary of *E. coli* detection rates during sampling campaigns in September 2012 and May to June 2013 at Hazzir spring. Detection rates are given in MPN 100 mL^{-1}. Dates of the sampling day are italic and numbers in brackets equal the measurement number of the day.

Day	Sunday		Monday	Tuesday	Wednesday	Thursday	Friday	Saturday
September 2012				*11th*	*12th*	*13th*	*14th*	*15th*
				326 (1)	152 (1)	649 (1)	816 (1)	579 (1)
				291 (2)	162 (2)	435 (2)	1.300 (2)	291 (2)
					179 (3)	579 (3)	579 (3)	345 (3)
						1.300 (4)		
	16th		*17th*	*18th*	*19th*			
	1.553 (1)	687 (4)	613 (1)	142 (1)	210 (1)			
	1.733 (2)	548 (5)	387 (2)					
	1.986 (3)	345 (6)						
	1.986 (4)							
May to June 2013			*27th*	*28th*	*29th*	*30th*	*31th*	*1st*
			54 (1)	179 (1)	186 (1)	44 (1)	179 (1)	228 (1)
			46 (2)			142 (2)	119 (2)	150 (2)
	2nd		*3rd*	*4th*	*5th*	*6th*	*7th*	*8th*
	3.076 (1)[a]		2.909 (1)[a]	1.986 (1)	727 (1)	238 (1)	102 (1)	196 (1)
	24.196 (2)[a]				866 (2)	172 (2)		152 (2)
	9th		*10th*	*11th*				
	770 (1)		12.033 (1)[a]	687 (1)				
	2.420 (2)[a]							

[a] Values exceed the upper limit (UDL) of detection at 2.420 MPN 100 mL^{-1}; samples were retested by dilution.

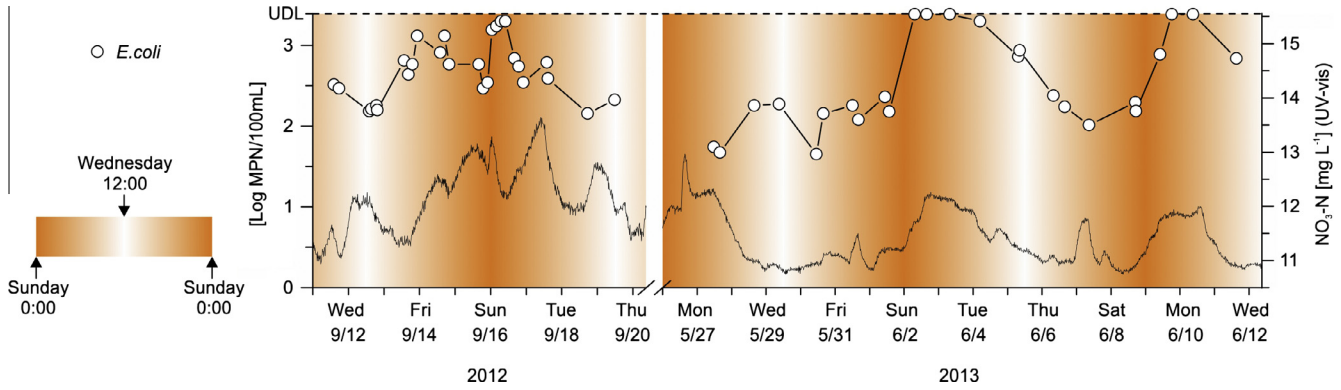

Fig. 6. Occurrence of *E. coli* at the Hazzir spring in September 2012 and May to June 2013. The abbreviation UDL represents the upper limit of detection of 2.420 MPN 100 mL^{-1}. The color gradient in the background visualizes the weekly pattern. (For interpretation of the references to color in this figure legend, the reader is referred to the web version of this article.)

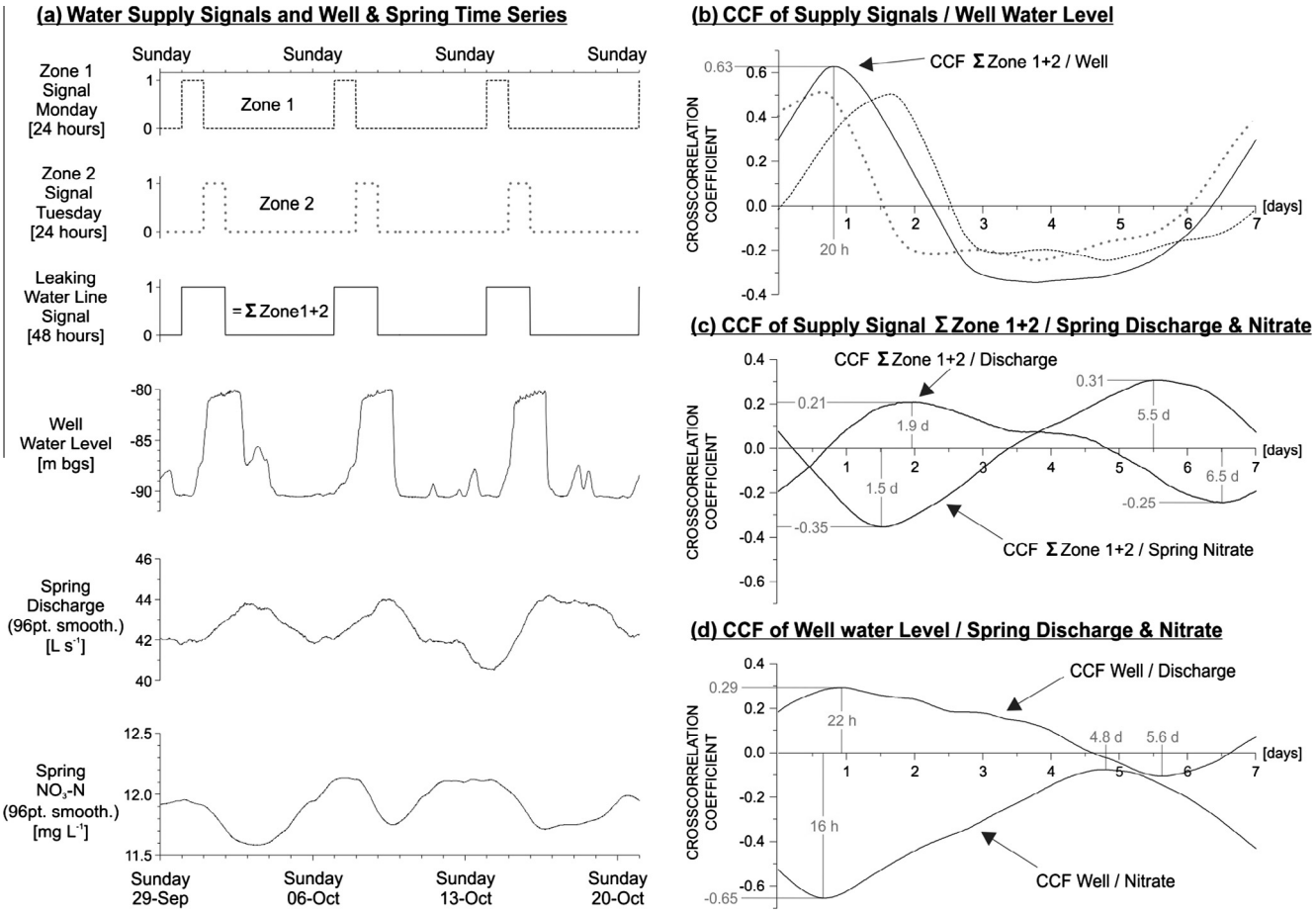

Fig. 7. (a) Three-week clip (29/09–21/10/2013; =22 days) of the observation well and spring time series beside an approximate and synchronized function representing intermittent water supply periods for zones 1 and 2, and the signal of the leaking water line near the well (=∑ zone 1 + 2). The *y*-axis of the weekly water supply signals corresponds to a value 0 for no flow in the water supply lines, and thus no leakage to the karst aquifer; the value 1 represents the weekly period for a functioning water supply, and thus leakage to the karst aquifer. (b–d) Cross-correlation functions (CCF) illustrated for a time lag until 7 days: (b) CCFs of zone 1 and well water level, zone 2 and well water level, and ∑ zone 1 + 2 and well water level. (c) CCFs of ∑ zone 1 + 2 and spring discharge, and ∑ zone 1 + 2 and spring nitrate. (d) CCFs of well water level and spring discharge, and well water level and spring nitrate.

these three supply signals in a three-week clip. Two signals refer both to a 24-h supply duration on Monday in zone 1 and Tuesday in zone 2, which are upgradient of the well and spring. The third signal refers to a 48-h duration and combination of zone 1 and 2 (Monday and Tuesday). This corresponds to the leaking water line next to the well which is pressurized during both supply times.

Cross-correlation functions (CCFs) were applied according to following procedure and assumptions:

(1) Each of the three water supply signals was cross-correlated with the well water level time series (=three CCFs; Fig. 7b). The CCFs are used to verify, which water supply signal

(24 or 48 h) fits better to the well water level time series. Accordingly higher positive or negative correlation and the corresponding delay of the weekly variation are assessed.

(2) Each water supply signal was cross-correlated with the spring discharge and spring nitrate time series (=six CCFs; Fig. 7c and Supplementary Fig. 2). The CCFs are used to verify which water supply signal fits best to the two spring time series, and the delays of the weekly variation between input and output signals are assessed. Subsequently, an evaluation of whether spring discharge and nitrate time series follow either a primary positive or negative correlation pattern is applied.

(3) The well water level time series was cross-correlated with the spring discharge and spring nitrate time series (=two CCFs; Fig. 7d). The CCFs are used to assess the general similarity between the time series, the delay of the weekly variation between input and output, and to compare the pattern of the two CCFs. This requires the assumption of a hydrologic connection between the well and the down-gradient spring.

- All CCFs were computed for the period from 09/06 to 04/11/2013 (=148 days).
- The assessment of derived CCFs applies only to lag times of the first week (=lag 0–7 days), because delays of the anthropogenic weekly impulse of more than one week, e.g. two or three weeks, are assumed to be unrealistic.

The application of cross-correlation analysis by using simplified water supply zone signals as systemic input cannot provide evidence concerning the origin of the observed periodicities because the weekly input signals have the same frequency and are only out of phase and therefore autocorrelated between each other. However, their use still allows a generally better characterization of an artificial impulse transfer in the local karst aquifer system.

The following results are derived by the three assessments (1)–(3):

(1) The CCFs between water supply signals and well time series show a better positive correlation with the 48-h signal (0.63 for $\sum$ Zone 1 + 2; Fig. 7b). A corresponding delay of about 20 h between the assumed leakage impulse and increasing water level can be detected.

(2) The CCFs between the 48-h signal and spring time series show higher coefficients (0.21 to −0.25 for discharge and −0.35 to 0.31 for nitrate; Fig. 7c) as compared with the 24 h signals (0.19 to −0.2 and −0.28 to 0.22; Supplementary Fig. 2). Therefore, the weekly fluctuations more likely result from a 48-h impulse. The two CCFs with 48-h signal show an opposing pattern, with similar negative and positive peaks and correlation coefficients. This opposing pattern indicates that weekly variations of spring discharge and nitrate concentration appear to be synchronized. Derived correlation coefficients of peaks are weaker compared to the well water level CCFs in (1), which most likely could result from a longer flow path through the aquifer system (increased attenuation of an impulse). Associated delay times of corresponding negative and positive peaks show an earlier weekly response of spring nitrate than for discharge (1.5 days and 1.9 days of first peaks or 5.5 days and 6.5 days of second peaks). A shorter delay of the nitrate signal's weekly variation compared to the discharge signal, seems reversed, since a pressure impulse is transferred faster than the chemical variation. Since the measuring points are slightly different, with the nitrate sensor inside the spring reservoir, and the discharge measurement outside and down-gradient of the reservoir, this could be a possible explanation for the difference. A slightly weaker significance of cross-correlation functions is derived by the CCF with spring discharge compared to the CCF with spring nitrate. This is due to the noisy signal of the discharge time series. By filtering the signal, this level of significance can be increased to similar values as computed for the nitrate time series, whereas delay times are nearly unchanged.

(3) The CCFs between well and spring nitrate time series show distinctively better correlation coefficients (−0.65) as the CCF of well and spring discharge time series (0.29; Fig. 7d). Both CCFs follow an opposing pattern. First peaks are considered significantly correlated and second peaks as well bot not significantly. The two corresponding delay times are at 16 h and 22 h. Similar to the second assessment (2) the nitrate time series lead to shorter delays as the CCF of spring discharge time series.

3.4.1. Interpretation of cross-correlations

(1) The assessment of the CCFs between different IWS durations (input signals) and the well water level showed best correlation with the 48-h signal. It gives a clear explanation of the influence of network losses from a leaking water line on the observation well. The weekly increasing potentiometric surface of the well is most likely linked with weekly percolation of leaking clean water from the major nearby line.

(2)–(3) The CCFs of spring discharge and nitrate correlated with simplified water supply signals (2) or correlated with the well water level time series (3) show a weekly opposing pattern with similar delay times for corresponding peaks. This inverse correlation demonstrates the weekly dilution and enhancement of spring water discharge. Decreasing nitrate concentrations are accompanied by an increasing spring discharge and vice versa. The weekly addition of leaking and infiltrating clean water dilutes the contaminated groundwater and induces a weekly fluctuation of the nitrate concentrations. Therefore, opposing correlation coefficients explain the impact of weekly dilution induced by the IWS. The opposing correlations can also be demonstrated by visual comparison of the raw time series, but the CCFs quantify and confirm this relationship. The observed pattern of *E. coli* (Section 3.3) with a positive correlation to nitrate and negative correlation to discharge confirms the dilution theory. No crucial delay of the *E. coli* compared to the discharge pattern was identified therefore the source of fecal contamination is not associated with the origin of the weekly impact.

According to Brown (1973) or Valdes et al. (2006) we assume a simple systematic response (well established input–output connection) of a conduit network connection wherein a short delay comes from the transmission of the pressure pulse through the saturated zone during low flow. The cross-correlation analyses of the spring time series illustrated the similarity with the well water time series and an approximated leaking water supply signal (48-h signal), strongly suggest a causative link with IWS. Although low flow conditions are investigated, the observed peak times of 16–22 h for the CCFs between well and spring would coincide well with the range of response times during rainfall events (20–24 h).

The derived peak times for the three CCF assessments (1)–(3) derived following (down-gradient) order of delays between the leaking water line, the well and the spring are as follows:

- 20 h delay of weekly variation between the leaking water line and the well,
- 1.5–1.9 days (about 36–46 h) delay of weekly variation between the leaking water line and the spring,

- and 16–22 h delay of weekly variation between the well and the spring.

The difference of delays between leaking water line and well (1) and leaking water line and spring (2), which corresponds also to the transfer direction from well to spring ('water line to spring' – 'water line to well' = 'well to spring'), is about 16–26 h. This would be consistent with the derived delay from the well to the spring (16–22 h). In summary, cross-correlation analyses reveal a transfer time between the well and spring of approximately one day or even less during low flow.

4. Conclusion

By means of high-resolution monitoring of well and spring hydro- and chemo-graphs, the hydrological dynamics of an urban karst aquifer were characterized during two dry periods. Water levels, discharge, nitrate and *E. coli* were used to confirm the general notion of complex intrakarstic contamination dynamics and the susceptibility of karst aquifers to urban impacts.

The results of this study add to existing knowledge about the temporal and cyclic evolution of the local groundwater contaminant concentrations and subsurface mixing processes in the area. Correlation analysis of the different time series lead to the conclusion that regular weekly variations of contaminant concentrations, discharge and water level are most likely driven by the systematic, areally-varying intermittent water supply (IWS) of the city upgradient from Hazzir Spring; most likely due to one major leakage of a water line nearby the well. Inverse correlation of nitrate and discharge are consistent with the continuous input of contaminants by leaking sewers which were further diluted by the weekly pulse of drinking water leaking from the IWS.

The use of time series with high temporal resolution, derived by spectrometric measurements, led to a better detection and understanding of contamination processes. The autocorrelation analysis was used to characterize the temporal variability of the aquifer system and although it is a simplified representation, the survey featured systematically recurring, anthropogenic components in the time series indicating an impulse-transfer in an active karst network.

As the weekly variation of the time series evidently does not describe the triggering mixing processes during the passage through the karstic network, we confirmed that cross-correlation analysis are useful to distinguish if dilution and mobilization processes are dominating. The approximation of the periodic IWS input signal allows investigating the impulse transfer through the karstic network. Furthermore, it shows that the spring discharge and nitrate time series are influenced by weekly dilution. This approach confirmed the occurrence of complex areal and temporal recharge to the karst aquifer from leaky infrastructure processes, wherein the impact of dilution by clean water from network losses and fecal contamination of sewer leakages are closely spaced. The results of this study advanced the knowledge about the complexity of an urban water cycle system with an IWS and can benefit water managers in Middle East. For sustainable water management, as well as for groundwater protection in regions of severe water scarcity, infrastructural measures such as modernization of mains and sewer systems are essential to reduce leakage from water-supply infrastructure.

Beside, water managers' benefits on a local scale, hydrologically-scheduled sampling strategies with high temporal resolution are crucial. Sewer rehabilitation and maintenance is equally important to reduce the continuous fecal contamination by leaking sewers. Specifically for the study area, water network losses of 50–60% in Wadi Shueib need to be reduced to help save valuable drinking water from contamination.

According to Pronk et al. (2009), short-term microbial contamination resulting from events (e.g. storms) can easily be detected by in-situ monitoring. On the other hand, in the long-term it is a challenge to assess water quality and its contamination variability. In terms of sampling strategies, the results of the fecal bacteria detection rates point out the major water management problem. The highest detection rates of coliforms occurred Sundays and Mondays, which allowed demonstration to the local water manager that a sampling protocol of only 2–3 days in a week, which is currently favored, is not representative enough to safeguard the public water supply. This insight on the weekly variability of *E. coli* detection rates led to alteration of the spring water supply of Hazzir spring and an advanced level of planning for groundwater use.

These results, the presented data and the statistical methods used herein point out the importance of high-resolution monitoring and the incorporation of quantitative tools that allow an advanced level of hydrogeologic understanding. Such approaches are essential, especially when environmental systems, such as As-Salt, with its complex urban water cycle, and its location in a highly vulnerable karstic aquifer in a semi-arid setting, are investigated or otherwise targeted for long-term protection and preservation.

Acknowledgements

This study was part of the SMART project funded by the German Federal Ministry of Education and Research (BMBF) (grant numbers: 02WM1079-1086, 02WM1211-1212). We thank Dr. Leif Wolf for his continued support. We are grateful to the Jordanian Ministry of Water and Irrigation (MWI) for cooperation throughout the project. We are grateful to Dr. Ali Sawarieh, Dr. Frank Wendler, Chen Zhao and Dr. Tanja Liesch for support and scientific discussions. Analyses were conducted in our laboratory with the help of Daniela Blank and Christine Roske-Stegemann. We thank Prof. Dr. David Drew and Prof. Dr. Tim Bechtel for proofreading different parts of this paper.

Appendix A. Supplementary material

Supplementary data associated with this article can be found, in the online version, at http://dx.doi.org/10.1016/j.jhydrol.2016.03.045.

References

Abu-Jaber, N.S., Aloosy, A.S.E., Ali, A.J., 1997. Determination of aquifer susceptibility to pollution using statistical analysis. Environ. Geol. 31 (1–2), 94–106. http://dx.doi.org/10.1007/s002540050168.

Abu-Shams, I., Rabadi, A., 2003. Commercialization and public–private partnership in Jordan. Int. J. Water Resour. Dev. 19 (2), 159–172.

Al-Charideh, A., 2011. Recharge rate estimation in the Mountain karst aquifer system of Figeh spring, Syria. Environ. Earth Sci. 65 (4), 1169–1178. http://dx.doi.org/10.1007/s12665-011-1365-5.

Al-Kharabsheh, N.M., Al-Kharabsheh, A.A., Ghnaim, O.M., 2013. Effect of septic tanks and agricultural wastes on springs' water quality deterioration in Wadi Shu'eib Catchment Area-Jordan. Jordan J. Agric. Sci. 9 (1) <http://journals.ju.edu.jo/JJAS/article/view/3647>.

Amiel, R.B., Grodek, T., Frumkin, A., 2010. Characterization of the hydrogeology of the sacred Gihon Spring, Jerusalem: a deteriorating urban karst spring. Hydrogeol. J. 18 (6), 1465–1479. http://dx.doi.org/10.1007/s10040-010-0600-6.

Atkinson, T.C., 1977. Diffuse flow and conduit flow in limestone terrain in the Mendip Hills, Somerset (Great Britain). J. Hydrol. 35 (1–2), 93–110. http://dx.doi.org/10.1016/0022-1694(77)90079-8.

Bakalowicz, M., El Hakim, M., El-Hajj, A., 2008. Karst groundwater resources in the countries of eastern Mediterranean: the example of Lebanon. Environ. Geol. 54 (3), 597–604. http://dx.doi.org/10.1007/s00254-007-0854-z.

Barrett, M.H., Hiscock, K.M., Pedley, S., Lerner, D.N., Tellam, J.H., French, M.J., 1999. Marker species for identifying urban groundwater recharge sources: a review and case study in Nottingham, UK. Water Res. 33 (14), 3083–3097. http://dx.doi.org/10.1016/S0043-1354(99)00021-4.

Bende-Michl, U., Hairsine, P.B., 2010. A systematic approach to choosing an automated nutrient analyser for river monitoring. J. Environ. Monit.: JEM 12 (1), 127–134. http://dx.doi.org/10.1039/b910156j.
Bender, F., 1968. Geologie von Jordanien. Beiträge zur regionalen Geologie der Erde. Gebrüder Bonträger, Berlin.
Bonn, T., 2013. Wasserpolitik in Jordanien, 9. LIT Verlag Münster.
Box, G., Jenkins, G., Reinsel, G., 1994. Time Series Analysis: Forecasting and Control. Prentice-Hall International.
Brown, M.C., 1973. Mass balance and spectral analysis applied to Karst hydrologie networks. Water Resour. Res. 9 (3), 749–752. http://dx.doi.org/10.1029/WR009i003p00749.
Daher, W., Pistre, S., Kneppers, A., Bakalowicz, M., Najem, W., 2011. Karst and artificial recharge: theoretical and practical problems: a preliminary approach to artificial recharge assessment. J. Hydrol. 408 (3–4), 189–202. http://dx.doi.org/10.1016/j.jhydrol.2011.07.017.
Davis, J.C., 2002. Statistics and Data Analysis in Geology, third ed. Wiley, New York.
Eiswirth, M., Wolf, L., Hotzl, H., 2004. Balancing the contaminant input into urban water resources. Environ. Geol. 46 (2), 246–256. http://dx.doi.org/10.1007/s00254-004-0981-8.
Fenech, C., Rock, L., Nolan, K., Tobin, J., Morrissey, A., 2012. The potential for a suite of isotope and chemical markers to differentiate sources of nitrate contamination: a review. Water Res. 46 (7), 2023–2041. http://dx.doi.org/10.1016/j.watres.2012.01.044.
Fiorillo, F., Doglioni, A., 2010. The relation between karst spring discharge and rainfall by cross-correlation analysis (Campania, southern Italy). Hydrogeol. J. 18 (8), 1881–1895. http://dx.doi.org/10.1007/s10040-010-0666-1.
Flexer, A., Yellin-Dror, A., 2008. Geology. In: Hötzl, H., Möller, P., Rosenthal, E. (Eds.), The Water of the Jordan Valley: Scarcity and Deterioration of Groundwater and Its Impact on the Regional Development. Springer (Chapter 2.1).
Ford, D., Williams, P.D., 2007. Karst Hydrogeology and Geomorphology. John Wiley & Sons.
Geyer, T., Birk, S., Liedl, R., Sauter, M., 2008. Quantification of temporal distribution of recharge in karst systems from spring hydrographs. J. Hydrol. 348 (3–4), 452–463. http://dx.doi.org/10.1016/j.jhydrol.2007.10.015.
Geyh, M.A., Rimawi, O., Udluft, P., Salameh, E., 1985. Environmental Isotope Study in the Hamad Region. Bundesanstalt fur Geowissenschaften und Rohstoffe und den Geologischen Landesamtern in der Bundesrepublik Deutschland.
Goldscheider, N., 2010. Delineation of spring protection zones. In: Kresic, N., Stevanovic, Z. (Eds.), Groundwater Hydrology of Springs. Butterworth-Heinemann, Boston, pp. 305–338, http://dx.doi.org/10.1016/B978-1-85617-502-9.00008-6 (Chapter 8).
Goris, A., 2012. Schneider Bautabellen fuer Ingenieure. Werner Verlag.
Gutierrez, F., Parise, M., De Waele, J., Jourde, H., 2014. A review on natural and human-induced geohazards and impacts in karst. Earth-Sci. Rev.
Hahne, K., Margane, A., Borgstedt, A., 2008. Geological and Tectonical Setting of the Upper Wadi Shuayb Catchment Area, Jordan. Technical Cooperation Project 'Groundwater Resources Management', Special Report No. 7, Hannover.
Hardoy, J.E., Mitlin, D., Satterthwaite, D., 2014. Environmental Problems in an Urbanizing World: Finding Solutions in Cities in Africa, Asia and Latin America. Routledge.
Hibbs, B.J., Sharp, J.M., 2012. Hydrogeological impacts of urbanization. Environ. Eng. Geosci. 18 (1), 3–24. http://dx.doi.org/10.2113/gseegeosci.18.1.3.
Huebsch, M., Fenton, O., Horan, B., Hennessy, D., Richards, K.G., Jordan, P., Goldscheider, N., Butscher, C., Blum, P., 2014. Mobilisation or dilution? Nitrate response of karst springs to high rainfall events. Hydrol. Earth Syst. Sci. 18 (11), 4423–4435. http://dx.doi.org/10.5194/hess-18-4423-2014.
Huebsch, M., Grimmeisen, F., Zemann, M., Fenton, O., Jordan, P., Sawarieh, A., Blum, P., Goldscheider, N., 2015. Technical note: field experiences using UV/VIS sensors for high-resolution monitoring of nitrate in groundwater. Hydrol. Earth Syst. Sci.
Katz, B.G., 2012. Nitrate contamination in Karst groundwater. In: White, W.B., Culver, D.C. (Eds.), Encyclopedia of Caves, second ed. Academic Press, Amsterdam, pp. 564–568, http://dx.doi.org/10.1016/B978-0-12-383832-2.00083-9.
Krockel, L., Schwotzer, G., Lehmann, H., Wieduwilt, T., 2011. Spectral optical monitoring of nitrate in inland and seawater with miniaturized optical components. Water Res. 45 (3), 1423–1431. http://dx.doi.org/10.1016/j.watres.2010.10.033.
Kumar, M.S.M., Manohar, U., Pallavi, M.R.M., Anjana, G.R., 2013. Urban water supply and management. J. Indian Inst. Sci. 93 (2), 295–317.
Kumpel, E., Nelson, K.L., 2013. Comparing microbial water quality in an intermittent and continuous piped water supply. Water Res. 47 (14), 5176–5188. http://dx.doi.org/10.1016/j.watres.2013.05.058.
Kumpel, E., Nelson, K.L., 2014. Mechanisms affecting water quality in an intermittent piped water supply. Environ. Sci. Technol. 48 (5), 2766–2775. http://dx.doi.org/10.1021/Es405054u.
Larocque, M., Mangin, A., Razack, M., Banton, O., 1998. Contribution of correlation and spectral analyses to the regional study of a large karst aquifer (Charente, France). J. Hydrol. 205 (3–4), 217–231. http://dx.doi.org/10.1016/S0022-1694(97)00155-8.
Lerner, D.N., 1986. Leaking pipes recharge groundwater. Ground Water 24 (5), 654–662. http://dx.doi.org/10.1111/j.1745-6584.1986.tb03714.x.
Lerner, D.N., 2002. Identifying and quantifying urban recharge: a review. Hydrogeol. J. 10 (1), 143–152. http://dx.doi.org/10.1007/s10040-001-0177-1.
Liu, L.H., Chen, X.H., Xu, G.Q., Shu, L.C., 2011. Use of hydrologic time-series data for identification of hydrodynamic function and behavior in a karstic water system in China. Hydrogeol. J. 19 (8), 1577–1585. http://dx.doi.org/10.1007/s10040-011-0774-6.
Mangin, A., 1984. Pour une meilleure connaissance des systèmes hydrologiques à partir des analyses corrélatoire et spectrale. J. Hydrol. 67 (1–4), 25–43. http://dx.doi.org/10.1016/0022-1694(84)90230-0.
Margane, A., Hobler, M., Almomani, M., Subah, A., 2002. Contributions to the Hydrogeology of Northern and Central Jordan. Hannover.
Margane, A., Subah, A., Hamdan, I., Hajali, Z., Almomani, T., 2010. Delineation of Groundwater Protection Zones for the Wadi Shuayb Springs. Technical Cooperation Project 'Groundwater Resources Management', Technical Report No. 14, Amman.
Margane, A., Zuhdy, M., 1995. Groundwater Resources of Northern Jordan, Part 1: Rainfall in Jordan. Technical Cooperation Project 'Advisory Services to the Water Authority of Jordan', vol. 1. BGR & WAJ, Amman.
Martinez, S.E., Escolero, O., Wolf, L., 2011. Total urban water cycle models in semiarid environments-quantitative scenario analysis at the area of San Luis Potosi, Mexico. Water Resour. Manage. 25 (1), 239–263. http://dx.doi.org/10.1007/s11269-010-9697-6.
Massei, N., Dupont, J.P., Mahler, B.J., Laignel, B., Fournier, M., Valdes, D., Ogier, S., 2006. Investigating transport properties and turbidity dynamics of a karst aquifer using correlation, spectral, and wavelet analyses. J. Hydrol. 329 (1–2), 244–257. http://dx.doi.org/10.1016/j.jhydrol.2006.02.021.
McIntosh, A.C., 2003. Asian Water Supplies: Reaching the Urban Poor: A Guide and Sourcebook on Urban Water Supplies in Asia for Governments, Utilities, Consultants, Development Agencies, and Nongovernment Organizations. Asian Development Bank.
Mimi, Z.A., Assi, A., 2009. Intrinsic vulnerability, hazard and risk mapping for karst aquifers: a case study. J. Hydrol. 364 (3–4), 298–310. http://dx.doi.org/10.1016/j.jhydrol.2008.11.008.
Moh'd, B.K., Muneuzel, S., 1998. The Geology of As Salt Area Map Sheet No. 3154 III. H.K. J. Nat. Res. Auth. Bulletin, No. 41, Amman.
MWI, GTZ, 2004. National Water Master Plan. Ministry of Water and Irrigation (MWI) & German Technical Cooperation (GTZ), Amman.
Padilla, A., Pulido-Bosch, A., 1995. Study of hydrographs of karstic aquifers by means of correlation and cross-spectral analysis. J. Hydrol. 168 (1–4), 73–89. http://dx.doi.org/10.1016/0022-1694(94)02648-U.
Panno, S.V., Hackley, K.C., Hwang, H.H., Kelly, W.R., 2001. Determination of the sources of nitrate contamination in karst springs using isotopic and chemical indicators. Chem. Geol. 179 (1–4), 113–128. http://dx.doi.org/10.1016/S0009-2541(01)00318-7.
Parker, D., 1970. Investigation of the Sandstone Aquifers of East Jordan. FAO.
Perfler, R., Langergraber, G., Lettl, W., Fleischmann, N., 2006. Use of UV–vis spectrometry for alarm parameters in drinking water supply. In: Pollert, J., Dedus, B. (Eds.), Security of Water Supply Systems: From Source to Tap. NATO Security through Science Series. Springer, Netherlands, pp. 85–98, http://dx.doi.org/10.1007/1-4020-4564-6_8.
Peterson, E.W., Davis, R.K., Brahana, J.V., Orndorff, H.A., 2002. Movement of nitrate through regolith covered karst terrane, northwest Arkansas. J. Hydrol. 256 (1–2), 35–47. http://dx.doi.org/10.1016/S0022-1694(01)00525-X.
Pronk, M., Goldscheider, N., Zopfi, J., 2006. Dynamics and interaction of organic carbon, turbidity and bacteria in a karst aquifer system. Hydrogeol. J. 14 (4), 473–484. http://dx.doi.org/10.1007/s10040-005-0454-5.
Pronk, M., Goldscheider, N., Zopfi, J., 2009. Microbial communities in karst groundwater and their potential use for biomonitoring. Hydrogeol. J. 17 (1), 37–48. http://dx.doi.org/10.1007/s10040-008-0350-x.
Rieger, L., Langergraber, G., Siegrist, H., 2006. Uncertainties of spectral in situ measurements in wastewater using different calibration approaches. Water Sci. Technol. 53 (12), 187. http://dx.doi.org/10.2166/wst.2006.421.
Riepl, D., 2012. Knowledge-Based Decision Support for Integrated Water Resources Management with an Application for Wadi Shueib. KIT Scientific Publishing, Jordan.
Rosenberg, D.E., Talozi, S., Lund, J.R., 2008. Intermittent water supplies: challenges and opportunities for residential water users in Jordan. Water Int. 33 (4), 488–504. http://dx.doi.org/10.1080/02508060802474574.
Rutsch, M., Rieckermann, J., Krebs, P., 2006. Quantification of sewer leakage: a review. Water Sci. Technol. 54 (6–7), 135. http://dx.doi.org/10.2166/wst.2006.616.
Schirmer, M., Leschik, S., Musolff, A., 2013. Current research in urban hydrogeology – a review. Adv. Water Resour. 51, 280–291. http://dx.doi.org/10.1016/j.advwatres.2012.06.015.
Schmidt, S., 2014. Hydrogeological Characterisation of Karst Aquifers in Semi-arid Environments at the Catchment Scale – Example of the Western Lower Jordan Valley. Georg-August-Universität Göttingen.
Schmidt, S., Geyer, T., Marei, A., Guttman, J., Sauter, M., 2013. Quantification of long-term wastewater impacts on karst groundwater resources in a semi-arid environment by chloride mass balance methods. J. Hydrol. 502, 177–190. http://dx.doi.org/10.1016/j.jhydrol.2013.08.009.
Slimani, S., Massei, N., Mesquita, J., Valdes, D., Fournier, M., Laignel, B., Dupont, J.P., 2009. Combined climatic and geological forcings on the spatio-temporal variability of piezometric levels in the chalk aquifer of Upper Normandy (France) at pluridecennal scale. Hydrogeol. J. 17 (8), 1823–1832. http://dx.doi.org/10.1007/s10040-009-0488-1.
Suleiman, R., 2004. The historical evolution of the water resources development in the Jordan river basin in Jordan. MREA-IWMI Working Paper. French Regional Mission for Water and Agriculture, Amman.

Ta'any, R., 1992. Hydrological and Hydrochemical Study of the Major Springs in Wadi Shu'eib Catchment Area, 302 pp.
Thompson, J., Porras, I.T., Tumwine, J.K., Mujwahuzi, M.R., Katui-Katua, M., Johnstone, N., Wood, L., 2002. Drawers of Water II. International Institute for Environment and Development, London.
Tokajian, S., Hashwa, F., 2003. Water quality problems associated with intermittent water supply. Water Sci. Technol. 47 (3), 229–234.
Toran, L., Reisch, C.E., 2013. Using stormwater hysteresis to characterize karst spring discharge. Ground Water 51 (4), 575–587. http://dx.doi.org/10.1111/j.1745-6584.2012.00984.x.
Vairavamoorthy, K., Gorantiwar, S.D., Pathirana, A., 2008. Managing urban water supplies in developing countries – climate change and water scarcity scenarios. Phys. Chem. Earth 33 (5), 330–339. http://dx.doi.org/10.1016/j.pce.2008.02.008.
Valdes, D., Dupont, J.P., Massei, N., Laignel, B., Rodet, J., 2006. Investigation of karst hydrodynamics and organization using autocorrelations and T–Delta C curves. J. Hydrol. 329 (3–4), 432–443. http://dx.doi.org/10.1016/j.jhydrol.2006.02.030.
Van Afferden, M., Cardona, J.A., Rahman, K.Z., Daoud, R., Headley, T., Kilani, Z., Subah, A., Mueller, R.A., 2010. A step towards decentralized wastewater management in the Lower Jordan Rift Valley. Water Sci. Technol. 61 (12), 3117–3128. http://dx.doi.org/10.2166/Wst.2010.234.
Vazquez-Sune, E., Carrera, J., Tubau, I., Sanchez-Vila, X., Soler, A., 2010. An approach to identify urban groundwater recharge. Hydrol. Earth Syst. Sci. 14 (10), 2085–2097. http://dx.doi.org/10.5194/hess-14-2085-2010.
Wakida, F.T., Lerner, D.N., 2005. Non-agricultural sources of groundwater nitrate: a review and case study. Water Res. 39 (1), 3–16. http://dx.doi.org/10.1016/j.watres.2004.07.026.
Werz, H., 2006. The Use of Remote Sensing Imagery for Groundwater Risk Intensity Mapping in the Wadi Shueib, Jordan.
White, W.B., 2002. Karst hydrology: recent developments and open questions. Eng. Geol. 65 (2–3), 85–105, pii: S0013-7952(01)00116-8.
Wolf, L., Held, I., Eiswirth, M., Hotzl, H., 2004. Impact of leaky sewers on groundwater quality. Acta Hydrochim. Hydrobiol. 32 (4–5), 361–373. http://dx.doi.org/10.1002/aheh.200400538.
Zemann, M., Wolf, L., Grimmeisen, F., Tiehm, A., Klinger, J., Hötzl, H., Goldscheider, N., 2015. Tracking changing X-ray contrast media application to an urban-influenced karst aquifer in the Wadi Shueib, Jordan. Environ. Pollut. 198, 133–143. http://dx.doi.org/10.1016/j.envpol.2014.11.033.
Zhang, Z.C., Chen, X., Chen, X.H., Shi, P., 2013. Quantifying time lag of epikarst-spring hydrograph response to rainfall using correlation and spectral analyses. Hydrogeol. J. 21 (7), 1619–1631. http://dx.doi.org/10.1007/s10040-013-1041-9.